MR. NORIAKI ARAI (Orcid ID : 0000-0002-3040-2997)

PROFESSOR KATHERINE T FABER (Orcid ID : 0000-0001-6585-2536)

Article type : Rapid Communication

ktfaber@caltech.edu

Freeze-Cast Honeycomb Structures via Gravity-Enhanced Convection

Noriaki Arai, Katherine T. Faber

Division of Engineering & Applied Science, California Institute of Technology,

Pasadena, CA, USA

Abstract

The effect of gravity on directional solidification was investigated in solution-based freeze casting. A preceramic siloxane-based polymer was freeze-cast with a cyclohexene solvent from two different directions: that against the direction of the gravitational force and that in concert with gravitational force. Since the density of preceramic polymer is higher than the solvent, the segregated polymer creates a denser solution ahead of the freezing front than the underlying solution when the freezing direction is the same as the gravity direction. This results in convective flow in the liquid phase. This convective flow influences constitutional supercooling, which changes not only the pore size of freeze-cast structure, but also the pore morphology from dendritic to cellular pores.

Introduction

Gravity is known to have a significant influence on materials processing. In float glass processing, a glass ribbon is produced by flowing molten glass on a molten tin bath[1]. With the help of gravity and surface tension, a flat glass with high surface quality can be fabricated. While this is an example where the presence of gravity is advantageous in material processing, some processing is negatively influenced by the gravitational force. In colloidal suspensions, sedimentation of particles by gravitational forces must be mitigated with suspension agents[2]. In another example, directional solidification for producing semiconductor crystals or nickel-based single crystals, gravity influences the convective flow in the melt. Since convection in the melt creates defects known as freckles in castings[3], solidification under microgravity[4] or with magnetic damping[5] has been explored to alleviate convection.

In this communication, we examine another processing method where gravity plays a role. Directional freeze casting is a porous material processing method which uses directional solidification as a means to create and control porosity and its orientation. In freeze casting, a suspension or solution is frozen such that growing crystals repel/segregate particles/solutes, and subsequent sublimation removes the crystals, leaving pores in the frozen body. Finally, the materials are sintered or pyrolyzed to produce porous solids. While pore morphologies can be controlled by the solvent choice[6], pore size can be controlled by the freezing front velocity and solid/solute loadings[7, 8]. The pore morphologies and pore size are known to affect the resulting mechanical properties and transport properties[7, 9]. Furthermore, improvement of these properties are possible by creating composites[10] or by improving the alignment of pores by nucleation control, such as with a grain selector[11].

Motivated by studies in directional solidification of metal alloys with convective flow[12–14], this study focuses on the effect of the convective flow induced by gravity during freeze casting. In alloy systems, depending on the density of the composition in alloys, convective flow may be present during directional solidification[15, 16]. For instance, in what has been labeled downward freezing (in the same direction as the gravitational force) if the solute is denser than the solvent, the segregated solute creates a denser fluid region ahead of the freezing front, and enhanced convective flow. In general, however, convection is limited to regions near the mold-alloy interface in upward freezing. Although the effect of gravity is actively studied in alloy solidification, a limited number of studies have examined gravity effects in freeze casting. Scotti et al. investigated the effect of the freezing direction with respect to gravity. Microstructures were found to contain tilted lamellar walls, ice lens formation

and radial micro-segregation, caused by the convective flow[17]. Another study demonstrated that different gravitational forces (micro-, lunar and Martian gravity) affect lamellar spacings[18]. Both however, were based on freeze-casting suspensions. Since suspensions are made up of particles and additives such as binders and dispersants, they are more complex systems compared to solutions, which contain only solutes and solvents. In this study, solidification was performed with solutions in both the conventional setup, where the gravitational force is opposite in direction than the freezing direction and a convection-enhanced setup, where the gravitational force is in concert with the freezing direction. The effect of enhanced convection induced by the gravitational force on solidification and the resulting porous structures are examined. In particular, the freezing front velocity and temperature gradient are compared between the two freezing conditions, and the resulting pore morphologies and pore sizes are investigated.

Experimental procedures

A preceramic polymer, polymethylsiloxane (Silres® MK Powder, Wacker Chemie, CH_3-$SiO_{1.5}$, Munich, Germany), was dissolved in cyclohexane (Sigma-Aldrich, St. Louis, MO, USA) at a concentration of 20 wt.%. A cross-linking agent (Geniosil® GF 91, Wacker Chemie, Munich, Germany) was added at a concentration of 1 wt.% with respect to the solution and stirred for 5 min. The polymer solution was degassed for 10 min to avoid air bubble formation during freezing. Directional freezing was conducted using a gradient-controlled freeze-casting setup[19]. The polymer solution was poured into a cylindrical mold placed on a thermoelectric plate. A second thermoelectric plate was placed on top of the mold, enabling control of freezing front velocity and temperature gradient. The sample was frozen in two different directions: one against the direction of gravity, referred as conventional freezing and one along the direction of gravity, referred to as convection-enhanced freezing (Figures 1a,b). The cooling profiles for two thermoelectric plates were programmed such that solidification took place with a freezing front velocity of 1.7 μm/s and a temperature gradient of 2.4 K/mm in conventional freezing. For the convection-enhanced freezing, the cooling profiles were switched between the upper and lower thermoelectric plates such that the freezing proceeded from top to the bottom. Images of freezing front were captured once each minute by a camera with an intervalometer. Image analysis was performed using ImageJ (National Institutes of Health) to determine the freezing front velocity. The temperature gradient was defined by:

$$G = \frac{T_{hot} - T_{front}}{d}$$

where T_{hot}, T_{front}, and d are the temperatures of the thermoelectric plate toward which the crystals are growing, the temperature at the freezing front, and the distance between points where T_{hot} and T_{front} are measured, respectively. The freezing front was assumed to be at the liquidus temperature reported by Naviroj[7]. The frozen samples were placed in a freeze drier to completely remove solvent crystals, and then pyrolyzed under argon at 1100 °C for 4 hours, resulting in porous silicon oxycarbide (SiOC). Porosity was measured using the Archimedes' method. Porous structures were imaged using scanning electron microscopy (SEM; ZEISS 1550VP, Carl Zeiss AG, Oberkochen, Germany), and pore sizes were determined by mercury intrusion porosimetry (MIP; AutoPoreIV, Micromeritics, Norcross, GA, USA).

Results

Figure 1c shows the freezing front position (FFP) with respect to the nucleation side as a function of time. Conventional freezing shows a nearly linear increase with time indicative of a constant freezing front velocity; moreover, the freezing front is planar (Figure 1d). In contrast, in convection-enhanced freezing, the FFP gradually increases for approximately 50 min, followed by the sudden increase in slope, representing a distinct increase in freezing front velocity, and the planar freezing front is deformed (Figure 1e). Between 45 and 47 min, the freezing front retracts, indicative of re-melting of the frozen solid. This behavior is shown in Figures 1e,f. Figure 1g illustrates the freezing front velocity and temperature gradient as a function of FFP from the nucleation side. Both freezing front velocity and temperature gradient remained nearly constant in conventional freezing, while in convection-enhanced freezing, show a large variation. Specifically, the freezing front velocity during its first four millimeters slows to the point of arresting and then becomes negative, where the freezing front re-melts, with the average freezing front velocity being ~0.7 μm/s. After four millimeters, the freezing front velocity suddenly increases, and exceeds the average freezing front velocity of conventional freezing.

Figures 2 displays SEM images in transverse directions (cross-sections perpendicular to the freezing direction), and longitudinal directions (cross-sections parallel to the freezing direction). The transverse images were taken from two different regions: a cross-section with FFP of ~1.6 mm and

~5 mm from the nucleation point. The longitudinal images of the conventional freeze-cast sample and the convection-enhanced freeze-cast sample are shown in Figures 2c,f, respectively, with the nucleation face indicated by red lines. In the conventional freeze-cast samples (Figures 2a-c), the pore morphologies are mainly dendritic structures, which consist of primary pores templated by primary dendrites and secondary pores templated by dendritic secondary arms, and the pore size is relatively consistent between the two regions (Figure 2a,b). In the longitudinal image, the first several hundred micrometers consist of a cellular region but the remaining pores are dendritic (Figure 2c). In stark contrast, the convection-enhanced freeze-cast sample shows cellular pores, which result in honeycomb-like structures, in the slow freezing region (FFP = ~1.6 mm, Figure 2d) while the fast freezing region (FFP = ~5 mm) exhibits dendritic structures (Figure 2e). The longitudinal image shows that the majority of pores (over more than 2 millimeters) are cellular pores (Figure 2f). The comparison of images between Figures 2a-c and Figures 2d-f indicates that the pore size derived from convection-enhanced freezing is smaller than that from conventional freezing.

Two specimens for porosimetry were sectioned from each sample and imaged; one near the nucleation region (FFP is around from 0.8mm to 3.3mm in Figure 1g – referred to as the nucleation section), and another from the middle section (FFP is around from 4.5mm to 7mm in Figure 1g – referred to as the middle section). Figure 3a compares the pore size distributions of the specimens sectioned from the nucleation section from two freezing conditions. A bimodal distribution can be observed in the conventional freeze-cast sample. Larger and smaller pores correspond to primary pores and secondary pores, respectively. In contrast, the convection-enhanced freeze-cast sample demonstrates a unimodal distribution, consistent with the SEM images (Figures 2d,f) showing a honeycomb-like structure. Figure 3b shows pore size distributions of specimens sectioned from the middle section. In this region, both samples display bimodal distributions as seen in SEM images (Figures 2b,e). Furthermore, the pore sizes are larger for conventional freeze-cast samples, again consistent with the SEM observations.

Discussion

As shown in Figures 1d,e, the conventional freezing yielded a planar freezing front while convection-enhanced freezing reveals a protruded freezing front. The difference can be attributed to the convective flow caused by the density variation in the liquid phase. This is a result of the

concentration gradients of preceramic polymer and temperature gradient in the liquid phase. Figures 4a,b are schematics of temperature and concentration variation in the liquid region. In conventional freezing, the preceramic polymer is segregated just ahead of the freezing front, resulting in a higher concentration of preceramic polymer at the freezing front, decaying into the liquid region. Since the segregated preceramic polymer (~1.26 g/cm^3) is denser than cyclohexane (~ 0.78 g/cm^3), the underlying liquid is heavier than that above. In addition, the region near the freezing front is colder than the overlying liquid. Since the density of the underlying liquid is higher, conventional freezing is a convectively stable configuration (Figure 4a). In the case of convection-enhanced freezing, the density gradient is reversed, therefore, leading to convective flow ahead of the freezing front (Figure 4b). Under such conditions, upwelling and downwelling currents are created, shown schematically in Figure 4c. The preceramic polymer is depleted above the upwelling current which gives rise to a crest, whereas the preceramic polymer is rich above downwelling current, which produces a trough, similar to the case reported by Drevet et al.[15]. As a result, the freezing front is deformed, consistent with the observation in Figure 1e. Remelting of the freezing front (the crest) was also observed (Figure 1f). A possible explanation is that the continuous convective flow transporting heat from the bottom to the top could remelt the frozen region.

While conventional freezing yielded nearly constant freezing front velocities and temperature gradients, that was not the case for convection-enhanced freezing. This discrepancy in freezing front velocity between conventional freezing and convection-enhanced freezing can be explained by constitutional supercooling of the solution. Due to convective flow, the solute is transported away from the solid-liquid interface and heat is transported toward the solid-liquid interface in convection-enhanced freezing, decreasing the degree of constitutional supercooling and lowering the driving force for crystal growth. As a result, the freezing front velocity initially remains slow (Figure 1g). However, as shown in the same figure, as the temperature gradient continues to decrease, the degree of the constitutional supercooling increases. This leads to a larger driving force for dendritic growth, and the freezing front velocity increases.

It is important to note that convective instabilities change both pore size and morphology. In conventional freeze-cast samples, the freezing front velocity and temperature gradient remain nearly constant, such that the pore structures and pore sizes remain similar between the nucleation section and middle section (Figures 3a,b). Since pore structures in the nucleation section and middle section are dendritic (Figures 2a,b), the pore size distributions are bimodal. It is worth noting that the primary

pore volume fraction in the nucleation section, represented by a larger incremental intrusion for primary pores, is larger than the one in the middle section. This is likely due to the presence of cellular pores found at the nucleation site and several hundred micrometers onward, as shown in the longitudinal image (Figure 2c). These pores are templated by cellular growth which is expected in the initial stages of the dendrite growth. As the freezing front advances as a flat interface, the interface is destabilized by the Mullins-Sekerka instability[20], leading to the transition from a flat interface to cells and eventually to dendrites. This transition is also observed in another freeze-casting study by Deville et al[21]. In contrast, convection-enhanced freezing leads to the long-range cellular regions as shown in Figure 2f, exhibiting a similar microstructure reported in other studies [22, 23]. The theory of constitutional supercooling is a useful tool to explain cellular growth in convection-enhanced freezing. Figure 4d shows a stability-microstructure map, which shows that cellular morphologies are formed only in a narrow region of slow freezing front velocities and high temperature gradients. Two possible factors are considered to explain the cellular morphology. The first is slower velocities (0.6~0.7 μm/s at 1.9 K/mm) as shown in Figure 1g. With the slower freezing front velocity, one would advance to the left in the stability-microstructure map in which cellular growth is expected (indicated by an orange arrow in Figure 4d). This is demonstrated by Zeng et al. who observed cellular pores by decreasing the freezing front velocity at constant temperature gradient[19]. However, this could not be the sole factor for the formation of the cells because the sample frozen under 0.7 μm/s and 4.9 K/mm with conventional freezing still exhibits dendritic pores with a bimodal pore size distribution (Figure 4e). A second consideration is the effect of convective flow on constitutional supercooling. Convective flow in convection-enhanced freezing drives the solute transport away from the freezing front, and this effect on constitutional supercooling can be described using a stability criterion for a stable planar freezing front[24]:

$$\frac{G}{V} = \frac{mC_0 1 - k_0}{D_L \quad k_0}$$

where G, V, m, C_0, D_L, and k_0 are temperature gradient, freezing front velocity, liquidus slope, concentration of the solution, the diffusion coefficient of the solute in the liquid, and equilibrium distribution coefficient, respectively. This equation defines the critical ratio, $^{G}/_{V}$, which ensures no constitutional supercooling, and defines the boundary between stable planar front and cellular growth in Figure 4d. Based on this equation, a higher diffusion coefficient provides a less stringent criterion to achieve a planar front. While it is only diffusion which transports solute away from the freezing

front in conventional freezing, convection further enhances the transport of solute in convection-enhanced freezing. As a result, the critical ratio for convection-enhanced freezing becomes less stringent, which makes cellular growth easier to attain, and cells crystallize instead of dendrites. Furthermore, the convective flow increases the temperature of the liquid phase near the solid-liquid interface, which can increase the local temperature gradient such that it is higher than the linear temperature gradient assumed in this study ($G = T_{hot} - T_{front}/d$). This would also contribute to a reduction in the degree of constitutional supercooling[4] and cells are more likely to grow.

To assess the length scale of the preceramic polymer transport by convection, the porosity of the conventional freeze-cast samples and convection-enhanced freeze-cast samples are measured. Four specimens each with a thickness of ~1.6 mm (corresponding to ~2.5 mm in the liquid phase) were sectioned from each pyrolyzed sample (#1, #2, #3 and #4). The specimen close to nucleation side is referred to as #1 whereas the specimen furthest from the nucleation side is referred to as #4. In order to show porosity variations within each sample, the difference in porosity between a section close to nucleation side (#1) and that of other three sections (#2, #3, and #4) are reported in Figure 4f. The differences are approximately $\pm$ 1 %, and no consistent trend can be observed in either freezing direction. It is likely that the variation in porosity is due to the measurement error in the Archimedes' method. This implies that the distance over which the preceramic polymer is transported by convection during convection-enhanced freezing is less than 2.5 mm in the solution. Even though transport of the solute appears to be limited to the near vicinity of the freezing front rather than throughout the entire liquid phase, constitutional supercooling is known to take place just ahead of the solid-liquid interface. Hence, even local solute transport reduces the degree of the constitutional supercooling, resulting in morphological and size changes of dendritic pores.

Conclusion

The effect of freezing direction with respect to the direction of the gravitational force was investigated in solution-based freeze casting. Two freezing directions were examined: conventional freezing, against the gravitational force, and convection-enhanced freezing, in concert with it. While conventional freezing allows a convectively stable configuration in the liquid phase, convection-enhanced freezing leads to convective instability. Convection in the liquid phase gives rise to transport of the preceramic polymer as well as heat in the vicinity of the solid-liquid interface. Due to

the reduced degree of constitutional supercooling in convection-enhanced freezing, a long-range honeycomb-like pore structure results and the pore size decreases. Hence, the understanding of convective flow in the liquid phase during freeze casting allows further control of pore morphology and pore size.

Acknowledgement

This work was supported by the National Science Foundation under CBET-1911972, and the Rothenberg Innovation Initiative (RI^2) program at Caltech.

The authors would like to thank Peter W. Voorhees for valuable advice and useful discussions of this work.

References

1. Pilkington LAB. Review Lecture: The float glass process. *Proc R Soc London A Math Phys Sci*. 1969;314(1516):1–25. https://doi.org/10.1098/rspa.1969.0212
2. Lewis JA. Colloidal processing of ceramics. *J Am Ceram Soc*. 2000;83(10):2341–2359. https://doi.org/10.1111/j.1151-2916.2000.tb01560.x
3. Copley SM, Giamei AF, Johnson SM, Hornbecker MF. The origin of freckles in unidirectionally solidified castings. *Metall Trans*. 1970;1(8):2193–2204. https://doi.org/10.1007/BF02643435
4. Jansen R, Sahm PR. Solidification under microgravity. *Mater Sci Eng*. 1984;65(1):199–212. https://doi.org/10.1016/0025-5416(84)90213-1
5. Prescott PJ, Incropera FP. Magnetically damped convection during solidification of a binary metal alloy. *J Heat Transfer*. 1993;115(2):302–310. https://doi.org/10.1115/1.2910680
6. Naviroj M, Voorhees PW, Faber KT. Suspension- and solution-based freeze casting for porous ceramics. *J Mater Res*. 2017;32(17):3372–3382. https://doi.org/10.1557/jmr.2017.133
7. Maninpat Naviroj. Silicon-based Porous Ceramics via Freeze Casting of Preceramic Polymers (Ph.D. thesis). Northwestern University; 2017
8. Macchetta A, Turner IG, Bowen CR. Fabrication of HA/TCP scaffolds with a graded and porous structure using a camphene-based freeze-casting method. *Acta Biomater*.

2009;5(4):1319–1327. https://doi.org/10.1016/j.actbio.2008.11.009

9. Arai N, Faber KT. Hierarchical porous ceramics via two-stage freeze casting of preceramic polymers. *Scr Mater*. 2019;162:72–76. https://doi.org/10.1016/j.scriptamat.2018.10.037

10. Kuo CT, Faber KT. Permeable carbon nanotube-reinforced silicon oxycarbide via freeze casting with enhanced mechanical stability. *J Eur Ceram Soc*. 2020;40(6):2470–2479. https://doi.org/10.1016/j.jeurceramsoc.2019.12.059

11. Naviroj M, Wang MM, Johnson MT, Faber KT. Nucleation-controlled freeze casting of preceramic polymers for uniaxial pores in Si-based ceramics. *Scr Mater*. 2017;130:32–36. https://doi.org/10.1016/j.scriptamat.2016.10.038

12. Spinelli JE, Rosa DM, Ferreira IL, Garcia A. Influence of melt convection on dendritic spacings of downward unsteady-state directionally solidified Al-Cu alloys. *Mater Sci Eng A*. 2004;383(2):271–282. https://doi.org/10.1016/j.msea.2004.06.021

13. Spinelli JE, Ferreira IL, Garcia A. Influence of melt convection on the columnar to equiaxed transition and microstructure of downward unsteady-state directionally solidified Sn-Pb alloys. *J Alloys Compd*. 2004;384(1–2):217–226. https://doi.org/10.1016/j.jallcom.2004.04.098

14. Shevchenko N, Boden S, Gerbeth G, Eckert S. Chimney Formation in Solidifying Ga-25wt pct In Alloys Under the Influence of Thermosolutal Melt Convection. *Metall Mater Trans A*. 2013;44A:3797–3808. https://doi.org/10.1007/s11661-013-1711-1

15. Drevet B, Nguyen Thi H, Camel D, Billia B, Dupouy MD. Solidification of aluminum-lithium alloys near the cell/dendrite transition-influence of solutal convection. *J Cryst Growth*. 2000;218(2):419–433. https://doi.org/10.1016/S0022-0248(00)00567-4

16. Spinelli JE, Rocha OFL, Garcia A. The influence of melt convection on dendritic spacing of downward unsteady-state directionally solidified Sn-Pb alloys. *Mater Res*. 2006;9(1):51–57. https://doi.org/10.1590/S1516-14392006000100011

17. Scotti KL, Kearney LG, Burns J, *et al.* The effect of solidification direction with respect to gravity on ice-templated TiO 2 microstructures. *J Eur Ceram Soc*. 2019;39(10):3180–3193. https://doi.org/10.1016/j.jeurceramsoc.2019.04.007

18. Scotti KL, Northard EE, Plunk A, Tappan BC, Dunand DC. Directional solidification of aqueous

TiO2 suspensions under reduced gravity. *Acta Mater*. 2017;124:608–619. https://doi.org/10.1016/j.actamat.2016.11.038

19. Zeng X, Arai N, Faber KT. Robust Cellular Shape-Memory Ceramics via Gradient-Controlled Freeze Casting. *Adv Eng Mater*. 2019;21(12):1900398. https://doi.org/10.1002/adem.201900398

20. Mullins WW, Sekerka RF. Stability of a Planar Interface During Solidification of a Dilute Binary Alloy. *J Appl Phys*. 1964;35(2):444. https://doi.org/10.1063/1.1713333

21. Deville S, Saiz E, Tomsia AP. Ice-templated porous alumina structures. *Acta Mater*. 2007;55(6):1965–1974. https://doi.org/10.1016/j.actamat.2006.11.003

22. Fukushima M, Yoshizawa Y. Fabrication of Highly Porous Silica Thermal Insulators Prepared by Gelation-Freezing Route. *J Am Ceram Soc*. 2014;97(3):713–717. https://doi.org/10.1111/jace.12723

23. Fukushima M, Nakata M, Zhou Y, Ohji T, Yoshizawa Y ichi. Fabrication and properties of ultra highly porous silicon carbide by the gelation-freezing method. *J Eur Ceram Soc*. 2010;30(14):2889–2896. https://doi.org/10.1016/j.jeurceramsoc.2010.03.018

24. Tiller W., Jackson K., Rutter J., Chalmers B. The redistribution of solute atoms during the solidification of metals. *Acta Metall*. 1953;1(4):428–437. https://doi.org/10.1016/0001-6160(53)90126-6

Figure 1 Freeze-casting setup of (a) conventional freezing and (b) convection-enhanced freezing. (c) Freezing front position as a function of time with images of (d) the freezing front in conventional freezing, and in convection-enhanced freezing at (e) t = 45 min and (f) t = 47 min (Red dashed line indicates the freezing front), and (g) the associated freezing front velocity and temperature gradient as a function of freezing front position.

Figure 2 SEM images of conventional freeze-cast samples showing transverse images at (a) FFP is ~1.6 mm and (b) FFP is ~5 mm from nucleation face, and (c) longitudinal image. SEM images of convection-enhanced freeze-cast sample showing transverse images at (d) FFP is ~1.6 mm and (e) FFP is ~5 mm from nucleation face, and (f) longitudinal image. Yellow arrows indicate freezing direction, v, and gravity direction, g. Red lines in (c) and (f) indicate the nucleation face.

Figure 3 Pore size distribution data from (a) nucleation section and (b) middle section.

Figure 4 Illustrations showing temperature and concentration variation in (a) conventional freezing and (b) convection-enhanced freezing. (c) An illustration showing convective flow in liquid phase in convection-enhanced freezing. (d) Stability-microstructure map based on temperature gradient and freezing front velocity. (e) Pore size distribution of conventional freeze-cast sample frozen under 0.7 μm/s and 4.9 K/mm. (f) Porosity difference between specimen close to nucleation section and other three specimens. Three samples were investigated for each freezing direction.

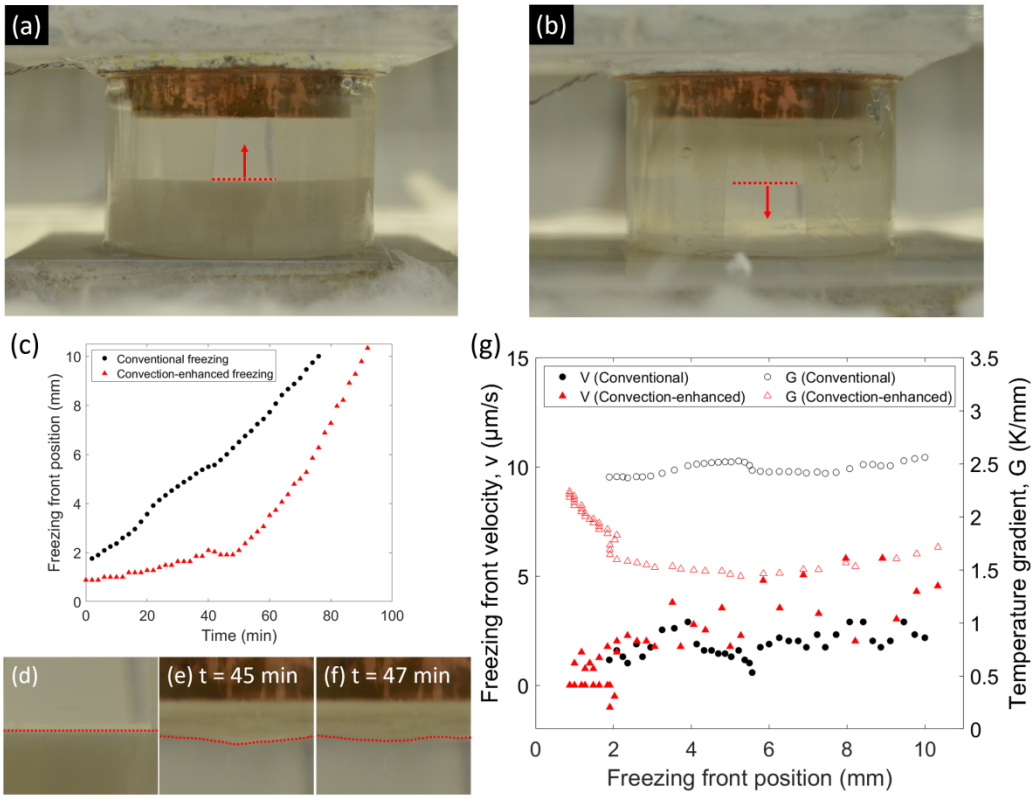

jace_17871_f1.tif

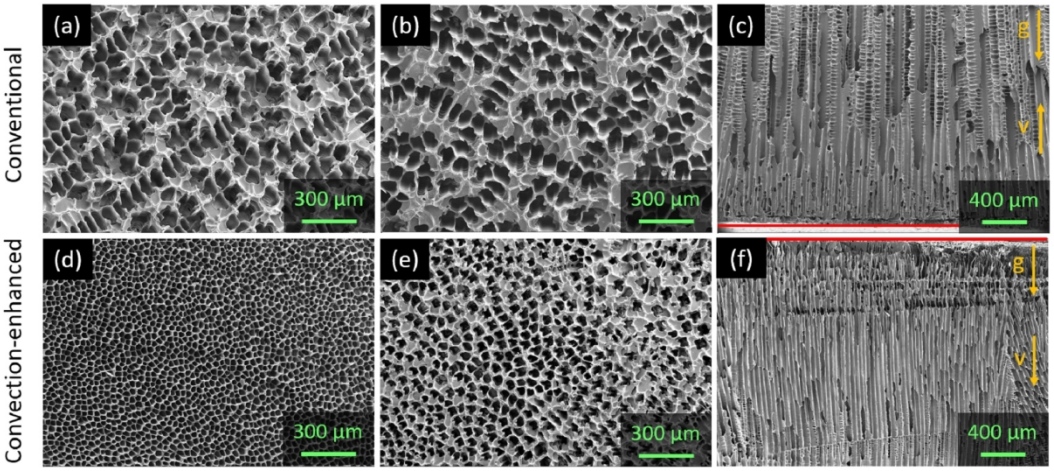

jace_17871_f2.jpg

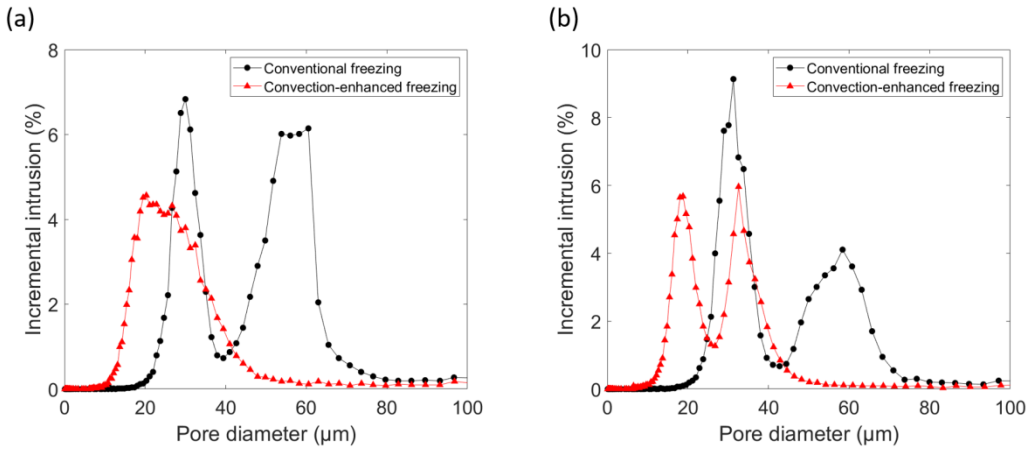

jace_17871_f3.tif

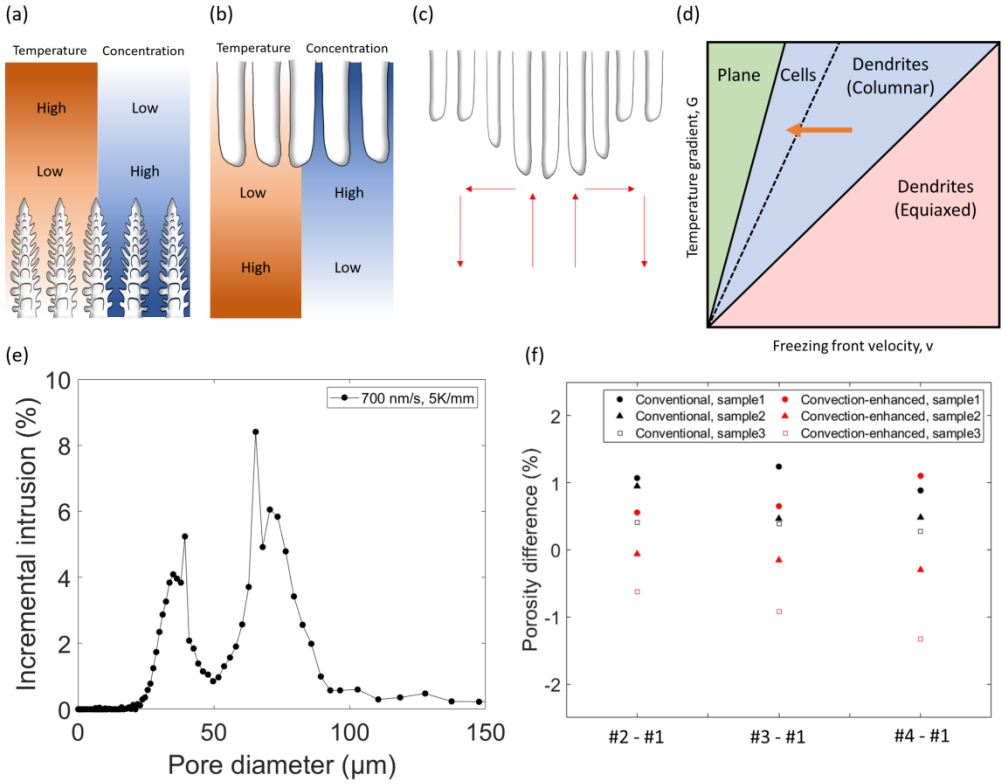

jace_17871_f4.tif